Gauge-including projector augmented-wave NMR chemical shift calculations with DFT+U

Bi-Ching Shih and Jonathan R. Yates
Department of Materials, University of Oxford, Parks Road, Oxford OX1 3PH, United Kingdom
(Received 18 February 2017; revised manuscript received 5 May 2017; published 27 July 2017)

We adapt the DFT+U method in the gauge-including projector augmented-wave NMR chemical shift calculations within the plane wave pseudopotential implementation. The nonlocal Hubbard correction potential has been reexamined in order to comply with the gauge-including projector augmented-wave transformation under an external uniform magnetic field. The resulting expression is suitable for chemical shift calculations using both norm-conserving and ultrasoft pseudopotentials in the proector augmented-wave scheme. The implementation is applied to the ^{17}O solid-state NMR chemical shift calculations for transition-metal and rare-earth oxides, including TiO_2, ZnO, Ti_2O_3, La_2O_3, and CeO_2. A comparison between the DFT and DFT+U NMR chemical shifts for the selected materials is presented.

DOI: 10.1103/PhysRevB.96.045142

I. INTRODUCTION

Nuclear magnetic resonance (NMR) spectroscopy has been one of the most powerful tools in determining and analyzing structural properties of materials in the atomic or molecular scale. Particularly, in the past two decades, the advances of solid-state NMR techniques, e.g., ultrahigh magnetic field and fast magic angle spinning frequency, have broadened the scope of studied materials and also prompted the research in this field. Besides, innovated NMR methodologies have also been devised which not only further enhance the power but also broaden the range and capacity of NMR spectroscopy. More comprehensive details of these experimental developments can be found in many review articles [1–6].

Despite the availability of unprecedented accuracy and resolution in NMR spectroscopy techniques having greatly improved and advanced the NMR measurements, the interpretation of NMR spectral data often resorts to the theoretical modeling calculations, particularly for solid-state systems. Early NMR experiments were usually analyzed by empirical methods and traditional quantum chemistry calculations; nevertheless, these approaches were only suitable or limited to simple or finite systems. Although it is possible to simulate solid-state NMR properties using the cluster approach, the calculations are usually inefficient for the large size of modeling systems and the results are insufficient for discounting the long range interactions in periodic systems. The introduction of gauge-including projector augmented-wave (GIPAW) NMR method [7] in this century has provided an effective theoretical approach to including the periodic effects in the solid-state NMR calculations.

The GIPAW NMR method [7] was first implemented based on the density functional theory [8,9] (DFT) in the plane wave norm-conserving pseudopotential scheme. The method provides all-electron level accuracy and has quickly become popular in the solid-state NMR field both in theoretical and experimental groups for predicting NMR parameters. Practically, it has been applied to a broad range of interested materials covering a majority of nuclei on the Periodic Table [5,10]. In terms of popularity, this method and its variants can be found in several computational packages (e.g., CASTEP [11], PARATEC [12], WIEN2K [13,14], GIPAW module in QUANTUM ESPRESSO [15] and VASP [16], etc.) Other frameworks of chemical shift calculations, e.g., the full potential method [17–19], the localized orbital method [20], and the converse approach [21], have also been implementated and documented. Methodologically, the functionality of the GIPAW method has also kept evolving and extending to evaluating other NMR parameters, such as hyperfine couplings [22,23], electric field gradients [24,25], and indirect couplings [26,27], etc.

Pragmatically, both the underlying DFT and the pseudopotential scheme pave the way to the success of the GIPAW NMR method. A later improved version adapted with more efficient ultrasoft pseudopotentials [28] has greatly relieved the computational limitations in the norm-conserving version, allowing us to study larger systems or systems containing heavier nuclei. However, there are several well known defects beneath the approximations for the exchange-correlation energy functionals, e.g., the local density approximation [9] (LDA) and generalized gradient approximation [29] (GGA), in the DFT. The resulting problems, for instance, the band gap problem [30,31] and self-interaction error [32], are particularly serious in systems containing strongly localized $3d$ and $4f$ electrons. A comprehensive understanding of the influence of these problems on GIPAW NMR calculations is uncharted yet. In addition, it is an inevitable problem of the prospect of the GIPAW method for covering the NMR calculations towards all nuclei on the Periodic Table. A variety of advanced exchange-correction functionals, such as hybrid functionals, have been devised to overcome these problems in DFT. There have been attempts of using hybrid functionals to calculate chemical shifts implemented in the all-electron augmented plane-wave scheme [33]. Unfortunately, the calculation is computationally expensive and the result shows no favorable improvement compared to standard functionals.

The DFT+U method [34,35], an inexpensive but effective alternative, is commonly applied to studying strongly correlated materials containing localized electrons. It has been generally recognized that the mean-field-like property of LDA/GGA is more suitable to describe itinerant electrons than localized ones. A prominent example is the electronic description of insulating band gap for Mott-Hubbard insulators when comparing results between LDA/GGA and DFT+U: by replacing the correlation interactions among localized electrons with a Hubbard-type potential from those in LDA/GGA, the DFT+U prompts the separations between the upper

and lower Hubbard bands and hence significantly raises the energy gap [34]. The strength of the Hubbard potential is conveniently described by a parameter, Hubbard U (sometimes also exchange J, depending on their formulations). Most often, the Hubbard U is treated as an adjustable parameter, though it can also be determined from first principles calculations, e.g., the constrained-LDA [36–39], constrained-RPA [40–49], and linear response [50] methods. Due to its feature, in electronic calculations, DFT+U have been popularly utilized to improve the DFT band gap or obtain better description of the ground states. The DFT+U NMR chemical shift calculation has been presented before [33]; however, the implementation is based on all-electron scheme and there are no detailed derivations of related formulations.

In this work, we extend the GIPAW chemical shift method to including the DFT+U energy functional. We deliberately adapt the Hubbard correction potential in the GIPAW Hamiltonian and response current formalism for chemical shift calculations: similar to the nonlocal part of pseudopotentials, a gauge dependent phase has to be included in the formulation of the nonlocal Hubbard correction potential due to the presence of a constant external magnetic field. A brief review of the GIPAW method is first presented followed by the required modifications for including the DFT+U in the GIPAW Hamiltonian and response current formulations. The implementation is demonstrated by studying the ^{17}O NMR chemical shifts in TiO_2 polymorphs, ZnO, Ti_2O_3, La_2O_3, and CeO_2. Some supplemental numerical validations for the GIPAW DFT+U implementation are provided in the Appendixes.

II. THEORY AND IMPLEMENTATION

In DFT electronic structure calculations, the inclusion of the Hubbard correction potential usually introduces dramatic changes on the electronic structures and sometimes also on the geometric structures when comparing them with those calculated using standard exchange-correlation potentials. It is expected that this correction potential shall have significant effects on the corresponding calculated NMR chemical shifts. In this section, we first recapitulate the key elements of the GIPAW chemical shift formulation within the LDA/GGA and then derive the corresponding adjustments required for DFT+U chemical shift calculations. The modifications of including the Hubbard term in the NMR formulations are alike between the norm-conserving and ultrasoft versions. Therefore, for simplicity, the following discussions will be demonstrated in the norm-conserving fashion only. However, wherever applicable, we will point out the crucial differences between the norm-conserving and ultrasoft formulations along the discussions.

A. Review of the GIPAW method

The original GIPAW NMR chemical shift calculation [7,28] for solids is implemented in the plane wave pseudopotential scheme based on the DFT. By calculating the induced current of the orbital electrons, the induced magnetic field can be conveniently evaluated according to the Biot-Savart law. The commonly defined chemical shielding can be obtained from the negative ratio between the induced and the external uniform magnetic fields, i.e., $\overleftrightarrow{\sigma} = -\mathbf{B}^{(1)}_{(\mathrm{in})}/\mathbf{B}$, which is a second-rank tensor. The relationship between the chemical shift and the chemical shielding will be described later. The calculation of induced currents requires the knowledge of the first order perturbed states which are calculated using density functional perturbation theory [51] (DFPT). There are two important ingredients in the GIPAW formulations of induction current calculations: (i) compensating the augmentation error due to the use of pseudopotentials and (ii) ensuring the Hamiltonian and other observable operators preserving the translational symmetry in a uniform external magnetic field. Upon the introduction of the GIPAW method, first by Pickard and Mauri [7], these requirements can be achieved simultaneously by imposing a translational invariant condition in the presence of a uniform magnetic field upon the projector augmented-wave (PAW) method [52].

It has been generally accepted that the PAW method bridges the pseudopotential method and augmented plane wave method [52]. While not only providing a scheme to restore the core-region wave functions, the PAW method also supplies a prescription for generating the pseudopotentials [52], which are separated into a local and a nonlocal part representing the ion-electron interaction potential, in the corresponding pseudo Hamiltonian. Fundamentally, these are achieved by the devised PAW transformation operator $\mathcal{T}^{\mathrm{PAW}}$ mapping softening pseudostates to their realistic all-electron states (near the core region), usually denoted as $|\psi\rangle = \mathcal{T}^{\mathrm{PAW}}|\tilde{\psi}\rangle$.

Although the PAW operator is able to serve as a candidate for restoring the wave functions in the core region, it does not preserve the translational symmetry when the system is in a uniform magnetic field. The cause of translational symmetry breaking in the PAW formulation originates from the so called gauge origin problem. However, it can be rectified by attaching a field dependent phase to the translated waves, as suggested in the GIPAW method. A similar idea can also be found in the gauge invariant atomic orbital (GIAO) approach [53] in the traditional quantum chemistry. Following the notations used in previous GIPAW papers [7,28], the GIPAW transformation operator is written as

$$\mathcal{T}^{\mathrm{GIPAW}} = \mathbf{1} + \sum_{\mathbf{R},n} e^{(i/c)\mathbf{A}(\mathbf{r})\cdot\mathbf{R}}[|\phi_{\mathbf{R},n}\rangle - |\tilde{\phi}_{\mathbf{R},n}\rangle] \times \langle \tilde{p}_{\mathbf{R},n}|e^{(-i/c)\mathbf{A}(\mathbf{r})\cdot\mathbf{R}}, \quad (1)$$

where $\mathbf{A}(\mathbf{r})$ is vector potential, $\mathbf{R}$ is the position of nuclei, n is the orbital quantum number of electrons, $\phi/\tilde{\phi}$ is the atomic/pseudoatomic orbital, and $\tilde{p}$ is the PAW projector. Now the GIPAW operator maps the magnetic pseudostates (GIPAW pseudostates) to the magnetic all-electron states by $|\psi\rangle_{\mathbf{B}} = \mathcal{T}^{\mathrm{GIPAW}}|\tilde{\psi}\rangle_{\mathbf{B}}$. For a local operator under GIPAW transformation, its GIPAW expression ($\bar{O}$) is related to its all-electron counterpart (O) by

$$\bar{O} = O + \sum_{\mathbf{R},n,m} e^{(i/c)\mathbf{A}(\mathbf{r})\cdot\mathbf{R}}|\tilde{p}_{\mathbf{R},n}\rangle \times [\langle\phi_{\mathbf{R},n}|e^{(-i/c)\mathbf{A}(\mathbf{r})\cdot\mathbf{R}} O\, e^{(i/c)\mathbf{A}(\mathbf{r})\cdot\mathbf{R}}|\phi_{\mathbf{R},m}\rangle - \langle\tilde{\phi}_{\mathbf{R},n}|e^{(-i/c)\mathbf{A}(\mathbf{r})\cdot\mathbf{R}} O\, e^{(i/c)\mathbf{A}(\mathbf{r})\cdot\mathbf{R}}|\tilde{\phi}_{\mathbf{R},m}\rangle] \times \langle\tilde{p}_{\mathbf{R},m}|e^{(-i/c)\mathbf{A}(\mathbf{r})\cdot\mathbf{R}}. \quad (2)$$

An alternative approach to elaborating the relationship between this extra phase and the translation symmetry is presented in Appendix A. Using the gauge-phase included PAW formulations, one can derive the GIPAW Hamiltonian and the GIPAW current density operator for the chemical shift calculation. For the details of the GIPAW induced current and chemical shift derivations and formulations, we refer readers to the literature [7,28] where either a norm-conserving or ultrasoft pseudopotential scheme is developed, suitable for the most commonly used local exchange-correlated potentials (e.g., the LDA or the GGA). At present, the core region is reconstructed to the all-electron atomic accuracy without considering the self-consistency.

B. GIPAW DFT+U Hamiltonian

Before properly including the Hubbard term in the NMR chemical shift calculations, we need to carefully examine the two issues described in the previous subsection for deriving the GIPAW DFT+U Hamiltonian. In regular DFT+U scheme without the presence of a magnetic field, the Hubbard potential can be concisely expressed in terms of the (all-electron) orbital projector operator [50]

$$V_{\mathrm{HUB}} = \sum_I V^I_{\mathrm{HUB}} = \sum_{I\sigma mm'} U^{I,\sigma}_{m,m'} |\varphi_{\mathbf{R}_I,m}\rangle\langle\varphi_{\mathbf{R}_I,m'}|, \tag{3}$$

where m (or m') denotes the atomic orbital quantum numbers of electrons, I is the index of targeted nuclei, σ is the spin index, and $|\varphi_{\mathbf{R}_I,m}\rangle$ indicates the (all-electron) d- or f-orbital functions centered at position $\mathbf{R}_I$ of a nucleus. The matrix elements $U^{I,\sigma}_{m,m'}$ are composed of occupation density matrix elements of a set of localized d or f orbitals and the screened Coulomb and exchange interaction parameters (usually denoted as U and J, respectively). Its explicit form depends on the specific DFT+U implementation and can be found in the literature [34,38,50,54,55]. It should be noted that the expression in Eq. (3) has included both a Hubbard-like interaction term and a double counting term. The orbital projector has to be properly revised when using pseudoatomic orbitals. Using the PAW transformation, we can express the pseudoversion of the PAW Hubbard potential

$$\begin{aligned}\tilde{V}_{\mathrm{HUB}} &= (\mathcal{T}^{\mathrm{PAW}})^\dagger V_{\mathrm{HUB}} \mathcal{T}^{\mathrm{PAW}} \\ &= \sum_{I\sigma mm'} U^{I,\sigma}_{m,m'} S^{(0)} |\tilde{\varphi}_{\mathbf{R}_I,m}\rangle\langle\tilde{\varphi}_{\mathbf{R}_I,m'}| S^{(0)},\end{aligned} \tag{4}$$

where the overlap operator $S^{(0)}$ is defined as

$$\begin{aligned}S^{(0)} &= (\mathcal{T}^{\mathrm{PAW}})^\dagger \mathcal{T}^{\mathrm{PAW}} \\ &= \mathbf{1} + \sum_{\mathbf{R},n,m} |\tilde{p}_{\mathbf{R},n}\rangle[\langle\phi_{\mathbf{R},n}|\phi_{\mathbf{R},m}\rangle - \langle\tilde{\phi}_{\mathbf{R},n}|\tilde{\phi}_{\mathbf{R},m}\rangle]\langle\tilde{p}_{\mathbf{R},m}|.\end{aligned} \tag{5}$$

For the norm-conserving version, the charge augmentation term in the square brackets is zero and the overlap operator returns to an identity operator. The derivations in Eq. (4) above have utilized the definitions of the PAW transformation $|\varphi\rangle = \mathcal{T}^{\mathrm{PAW}}|\tilde{\varphi}\rangle$ and the overlap operator literally. It should be noted that, unlike some PAW LDA+U formulations [56,57] where approximations have been used in deriving the pseudoversion of the projector operator, the expression of the PAW Hubbard potential in this article, which can also be seen in Ref. [58], doesn't resort to any approximation and is analytically exact.

In an environment with an external uniform magnetic field, both the PAW transformation operator and the Hubbard potential should have the forms which preserve the translational invariance property. In that case, the PAW transformation operator is replaced by the GIPAW operator and an additional phase has to be attached to the projector operator in the Hubbard potential. In short, the GIPAW Hubbard potential, expanded in powers of $\mathbf{B}$, can be written as

$$\begin{aligned}\bar{V}_{\mathrm{HUB}} &= (\mathcal{T}^{\mathrm{GIPAW}})^\dagger V_{\mathrm{HUB},\mathbf{B}} \mathcal{T}^{\mathrm{GIPAW}} \\ &\approx \tilde{V}_{\mathrm{HUB}} + \frac{1}{2c}\sum_I \mathbf{R}_I \times \frac{1}{i}\big[\mathbf{r}, \tilde{V}^I_{\mathrm{HUB}}\big]\cdot\mathbf{B}, \\ &\equiv \bar{V}^{(0)}_{\mathrm{HUB}} + \bar{V}^{(1)}_{\mathrm{HUB}},\end{aligned} \tag{6}$$

where the subscription $\mathbf{B}$ indicates the presence of the external magnetic field. Detailed derivations are presented in Appendix A.

With the Hubbard potential complying with the GIPAW scheme, the GIPAW transformed DFT+U Hamiltonian can be summarized as an unperturbed term

$$\bar{H}^{(0)} = \frac{1}{2}p^2 + V^{\mathrm{loc}} + \sum_{\mathbf{R}} V^{\mathrm{nl}}_{\mathbf{R}} + \sum_I \tilde{V}^I_{\mathrm{HUB}}, \tag{7}$$

and a first-order perturbed term

$$\begin{aligned}\bar{H}^{(1)} = \frac{1}{2c}\Bigg(&\mathbf{L} + \sum_{\mathbf{R}} \mathbf{R}\times\frac{1}{i}\big[\mathbf{r}, V^{\mathrm{nl}}_{\mathbf{R}}\big] \\ &+ \sum_I \mathbf{R}_I \times \frac{1}{i}[\mathbf{r}, \tilde{V}^I_{\mathrm{HUB}}]\Bigg)\cdot\mathbf{B},\end{aligned} \tag{8}$$

for the norm-conserving version [7]. An additional augmentation term from the angular momentum operator, which is not related to the Hubbard term, arises in the perturbed Hamiltonian in Eq. (8) for the ultrasoft case [28]. Compared to the standard (LDA/GGA) GIPAW Hamiltonian, the DFT+U GIPAW Hamiltonian includes an additional Hubbard potential in the unperturbed part and an extra term in the perturbed Hamiltonian contributed from the gauge phase, which preserves the transitional symmetry in the presence of a uniform magnetic field.

C. GIPAW DFT+U induced current

In this subsection, we discuss the required modifications of the induced current formulation when accommodating a GIPAW DFT+U calculation. From the DFT+U Hamiltonian developed in the previous subsection, a Hubbard correction term is required to be appended in both the unperturbed and the perturbed DFT Hamiltonian. These changes will also be contained in the DFT+U induced current expression implicitly.

To illustrate the changes in the calculation of the induced current with a DFT+U calculation, it is helpful to review the original GIPAW induced current formulations [7,28]. In the standard GIPAW NMR chemical shift method, the

gauge invariant kinematic momentum has been adopted in the definition of the orbital current density operator, $\mathbf{J}(\mathbf{r}') = -(\mathbf{p} + \frac{\mathbf{A}(\mathbf{r}')}{c})$, which includes a paramagnetic term and a diamagnetic term. This definition ensures the invariance of its expectation value regardless of the choice of gauge origin. The induced current in the GIPAW method is composed of a bare, a paramagnetic correction, and a diamagnetic correction term [7],

$$\mathbf{j}^{(1)}(\mathbf{r}') = \mathbf{j}^{(1)}_{\text{bare}}(\mathbf{r}') + \mathbf{j}^{(1)}_{\Delta\text{p}}(\mathbf{r}') + \mathbf{j}^{(1)}_{\Delta\text{d}}(\mathbf{r}'). \tag{9}$$

Three approaches have been developed for calculating the orbital induced current, including the molecular, molecular sum rule, and crystal approaches. The first two approaches are only suitable for finite systems such as molecules and the last approach has to be adopted for crystalline systems where the periodic conditions have been imposed on the formulation. We refer readers to the literature [7,28] for the detailed derivations and expressions of the three approaches.

For the norm-conserving version, as an example, the induced current in the molecular sum-rule approach is written as

$$\mathbf{j}^{(1)}_{\text{bare}}(\mathbf{r}') = 4\sum_{o} \text{Re}\Big[\big\langle\bar{\Psi}^{(0)}_o\big|\mathbf{J}^{\text{p}}(\mathbf{r}')\mathcal{G}\big(\varepsilon^{(0)}_o\big)\bar{H}^{(1)}\big|\bar{\Psi}^{(0)}_o\big\rangle - \big\langle\bar{\Psi}^{(0)}_o\big|\mathbf{J}^{\text{p}}(\mathbf{r}')\mathcal{G}\big(\varepsilon^{(0)}_o\big)\frac{\mathbf{B}\times\mathbf{r}'}{2c}\cdot\mathbf{v}\big|\bar{\Psi}^{(0)}_o\big\rangle\Big], \tag{10}$$

$$\mathbf{j}^{(1)}_{\Delta\text{p}}(\mathbf{r}') = 4\sum_{\mathbf{R}',o} \text{Re}\Big[\big\langle\bar{\Psi}^{(0)}_o\big|\Delta\mathbf{J}^{\text{p}}_{\mathbf{R}'}(\mathbf{r}')\mathcal{G}\big(\varepsilon^{(0)}_o\big)\bar{H}^{(1)}\big|\bar{\Psi}^{(0)}_o\big\rangle - \big\langle\bar{\Psi}^{(0)}_o\big|\Delta\mathbf{J}^{\text{p}}_{\mathbf{R}'}(\mathbf{r}')\mathcal{G}\big(\varepsilon^{(0)}_o\big)\frac{\mathbf{B}\times\mathbf{R}'}{2c}\cdot\mathbf{v}\big(\varepsilon^{(0)}_o\big)\big|\bar{\Psi}^{(0)}_o\big\rangle\Big], \tag{11}$$

and

$$\mathbf{j}^{(1)}_{\Delta\text{d}}(\mathbf{r}') = 2\sum_{\mathbf{R},o}\big\langle\bar{\Psi}^{(0)}_o\big|\Delta\mathbf{J}^{\text{d}}_{\mathbf{R}}(\mathbf{r}')\big|\bar{\Psi}^{(0)}_o\big\rangle, \tag{12}$$

where $\mathbf{v} = [\mathbf{r}, \bar{H}^{(0)} - \epsilon^{(0)}]/i$ is the (norm-conserving) velocity operator [7].

For the DFT+U formulation, by observing the operators in Eqs. (10)–(12), only the first-order perturbed Hamiltonian and the unperturbed Hamiltonian in the velocity operator appear in the bare and paramagnetic correction induced currents, i.e., Eqs. (10) and (11), which are required to be updated to the corresponding DFT+U version. The same conclusion can be made for the molecular and crystal approaches. For the ultrasoft case, the necessary steps of adapting the Hubbard potential to the induced current formula is exactly the same way as those in the norm-conserving case discussed above. A numerical validation for the DFT+U implementation is presented in Appendix B.

D. Implementation

Because of the resemblance of the formulations between the Hubbard correction potential and the PAW nonlocal pseudopotential, it is convenient to incorporate the Hubbard potential into the nonlocal pseudopotential, i.e., $V^{\text{nl}} \rightarrow V'^{\text{nl}} = V^{\text{nl}} + V_{\text{HUB}}$, in which the Hubbard potential is rewritten as $V_{\text{HUB}} = \sum_{\mathbf{R}} V^{\mathbf{R}}_{\text{HUB}}$ with nonzero terms only at a subset of ion sites $\mathbf{R}_I$ in mind. In this way, the DFT+U GIPAW NMR formulations are exactly the same as the original ones, except for an updated nonlocal potential term which includes the Hubbard correction term.

In practical implementations, we have adopted the Hubbard correction potential in the simplified rotational invariant version [50,55] with the double counting term in the form of the fully localized limit [59]. The potential strength in Eq. (3) is written as

$$U^{I,\sigma}_{m,m'} = U^I\left[\frac{\delta_{mm'}}{2} - n^{I\sigma}_{mm'}\right], \tag{13}$$

where $n^{I\sigma}_{mm'}$ is the occupation density matrix. In this expression, the effective Hubbard parameter U^I is related to the spherically averaged screened Coulomb interaction and screened exchange interaction by $U^I = U - J$ [55]. For the Hubbard potential, the basis functions of the projector operator are a set of pseudoatomic orbitals, while, for the nonlocal potential, they are a set of PAW projectors.

In the evaluation of the induced current, the velocity operator $\mathbf{v}$ is another essential operator required to be updated to the DFT+U version since it implicitly includes the Hubbard potential in the unperturbed Hamiltonian in the commutator. The position operator in the commutator is ill defined in the crystal method because of the periodic condition and can be conveniently transformed to a solvable modulation formalism [60]. An augmented version of the velocity operator should be used for the ultrasoft case [28]. A numerical validation of evaluating the DFT+U velocity operator and the equivalence of chemical shift calculations among three induced current approaches are presented in Appendix B.

Using the updated DFT+U induced current, the induced magnetic field at each nuclear site can be evaluated in the same way as described in previous GIPAW papers [7,28] and will not be repeated here. However, when evaluating the macroscopic susceptibility χ, which approximates (apart from a factor) the $\mathbf{G} = 0$ component of the bare induced field in the reciprocal space, the formulation involves a velocity operator and should be updated with the DFT+U version as well. Finally, the total chemical shift includes contributions from the induced field due to valence electrons plus the contribution from the core electrons which is treated as a nucleus-dependent constant [61].

III. CALCULATIONS AND RESULTS

The DFT+U is generally applied to strongly correlated materials for better electronic structures than those calculated with standard exchange-correlation functionals. Hence it is instructive to apply the newly implemented DFT+U GIPAW chemical shift calculations to materials containing localized $3d$ or $4f$ electrons. As the first test run of our implementation, it is instructive to target the relatively simple transition metal or rare-earth metal oxides where their experimental ^{17}O chemical shifts are available and reliable.

Early studies on ^{17}O chemical shieldings (or shifts) in silicates [25] and alkaline-earth metal oxides [62] have shown that the GIPAW (with the LDA or PBE [63] correlation functional) chemical shieldings are generally in good agreement with experimental measurements. The experimentally

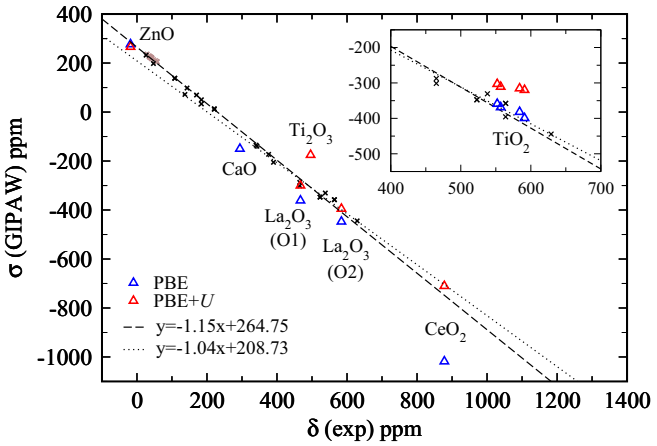

FIG. 1. Calculated ^{17}O NMR chemical shieldings in selected transition-metal and rare-earth oxides compared with experimental chemical shifts [65–68] and previous results (brown cross symbols for silicates [25] and black crosses for alkaline-earth oxides [62]). Present results are marked with the triangular symbols, colored in blue and red for PBE and PBE+U calculations, respectively. The dotted and dashed lines are linear regressions explained in the context.

measured chemical shift, δ, is related to the calculated isotropic chemical shielding, $\sigma_{\rm iso} = {\rm tr}(\sigma)/3$, by $\delta = \sigma_{\rm ref} - \sigma_{\rm iso}$, where $\sigma_{\rm ref}$ is the isotropic chemical shielding for a reference material. Because of the definition, it is straightforward to compare the experimental chemical shifts to the calculated chemical shieldings together with a linear regression analysis. In this way, the quality of GIPAW calculations can be measured by the slope of a regression line and corresponding deviations (e.g., the root mean square error). In practice, we expect that the DFT ^{17}O chemical shift for strongly correlated oxides might be deviated from the regression lines and a DFT+U calculation, with suitable material dependent U value, could bring the results back to the regression lines.

Based on the reasonings above, we study the ^{17}O NMR chemical shifts within the DFT/DFT+U for several $3d$- or $4f$-electron contained oxides, including TiO_2 polymorphs, ZnO, Ti_2O_3, La_2O_3, and CeO_2. The previously problematic case [64], CaO, is also revisited. The calculated isotropic chemical shieldings are compared with experimental chemical shifts as shown in Fig. 1. In the following context, we refer the term, chemical shielding, to the theoretically calculated quantities and chemical shift to experimental measurements in general. However, in some cases, where it is difficult to distinguish theoretical results or experimental data, only the chemical shift will be mentioned.

The DFT+U formulation for the GIPAW NMR chemical shielding calculation described in this work is implemented in CASTEP [11]. The ^{17}O NMR chemical shieldings in the aforementioned oxides are calculated with the PBE/PBE+U using the on-the-fly ultrasoft pseudopotential defined in CASTEP [11]. Particularly, for metallic ions, ($3d$, $4s$) electrons in Zn, ($3s$, $3p$, $3d$, $4s$) electrons in Ti, and ($4f$, $5s$, $5p$, $5d$, $6s$) electrons in La and Ce are treated as valence electrons. The chemical shieldings are calculated using the crystal approach with geometric structures optimized with respect to the PBE/PBE+U. The core contribution to the chemical shift is treated as rigid and is evaluated in the atomic code [61]. The plane wave cutoff energy and Monkhorst-Pack [69] **k**-point grids are chosen case by case so that the calculated shieldings are converged within 1 ppm for each oxide. Previous ^{17}O chemical shift results of silicates [25] and alkaline-earth oxides [62] are also reproduced in Fig. 1. Two regression lines are fitted as the reference for the presently studied materials. The regression line (a global fit) with a slope of -1.15 is obtained from results including all silicates and alkaline-earth metal oxides. Meanwhile, a second regression line (a local fit) with a slope of -1.04 is obtained from the data with experimental chemical shifts within 300 and 700 ppm. The slope of the second regression line indicates that, around the aforementioned range, earlier DFT GIPAW results agree with the experimental results very well and can be used as a standard reference for the present study.

We first revisit the problematic case of GIPAW calculated PBE ^{17}O chemical shielding for CaO. In the previous study [64] where the norm-conserving pseudopotential was used, it has shown that the large deviation (124 ppm) of the ^{17}O chemical shift for CaO is due to the improper description of the unoccupied Ca-$3d$ level. A tentative correction method has been proposed by imposing an upward shift on the Ca-$3d$ atomic energies without resorting to advanced exchange-correction potentials. We have reproduced the deviation, using the ultrasoft pseudopotentials instead, with the value of -150 ppm for the ^{17}O chemical shielding in CaO, compared to the previous -156.5 ppm using norm-conserving pseudopoetntails. As shown in Fig. 1, our value is 53–77 ppm below the two regression lines. Since the DFT+U can generally shift upward the unoccupied local orbital energies, it is expected that the DFT+U can be used to fix the overestimated ^{17}O chemical shift for CaO. Indeed, we have found that the chemical shift can be corrected within the two regression lines with the values of U between 1.14 and 1.62 eV for the Ca-$3d$ orbitals. When using the level shift method [64], a rigid shift on the Ca-$3d$ orbital energy between 1.08 and 1.88 eV is required instead.

In the next, we discuss ^{17}O chemical shielding results in transition-metal oxides. Among the selected materials, PBE produces reasonable ^{17}O chemical shieldings for ZnO (wurtzite phase) and TiO_2 polymorphs (rutile, anatase, and brookite phases) when compared to the global fit. For TiO_2 polymorphs, although the PBE+U has been commonly adopted for obtaining better energy gaps and optical spectra, their PBE ground states are generally considered reasonable in the standard DFT level due to their less localized and weaker correlated Ti $3d$ electrons. The latter argument is consistent with the present chemical shielding calculations where PBE results are in good agreement with the regression lines. For comparison, the PBE+U chemical shieldings calculated with $U = 4$ eV, which significantly deviate from the regression line, are also presented in the figure. The PBE chemical shift in ZnO, which locates closely at one of the regressions, is unexpected at first. In ZnO, it has been generally recognized that PBE severely underestimates the energy gap and the binding energies for Zn-$3d$ bands and overestimates the hybridization between O-$2p$ and Zn-$3d$ bands [70]. A PBE+U calculation with $U = 7$ eV applied to Zn-$3d$ orbitals is generally considered to be a better approach for obtaining a reasonable electronic ground state. The corresponding

chemical shielding moves away from the global fit by around only 8 ppm. The tiny shift after applying the Hubbard U is due to the forbidden linear response coupling between O-2p and Zn-3d bands where a similar mechanism has been explained in earlier chemical shift studies for sulfides [71]. As for Ti_2O_3 (corundum phase), a PBE shielding calculation is prohibitive since the PBE wrongly predicts a metallic phase in contradiction to an experimentally observed small energy gap of about 0.1 eV [72]. Although it is possible to open the band gap using the PBE+U with $U = 3$ eV, the resulting chemical shift strongly deviates from the regression, indicating that the Hubbard correction approach is not suitable for this material. The inadequacy of a pure DFT+U calculation for Ti_2O_3 can be related to its band gap formation [73–77]. For instance, a cluster LDA+DMFT study by Poteryaev *et al.* [75] indicates that the small energy gap is a result of the interplay of the strong bonding between the Ti-Ti pair and the correlations of the Hubbard potential.

For the rare-earth oxides, La_2O_3 (hexagonal phase) and CeO_2 (fluorite phase), the PBE+U method is required to attain results in line with the regressions. In La_2O_3, there are two inequivalent oxygen sites, one octahedrally coordinated (O1) and the other tetrahedrally coordinated (O2). Based on the relative values of the chemical shieldings either with the PBE or the PBE+U method, the experimental and theoretical assignments of the two inequivalent oxygen sites agree with each other. Relative to the local fit, the deviations of chemical shifts, −21 (O1) and 4 (O2) ppm, obtained from the PBE+U with $U = 2$ eV, are greatly improved from those of PBE's, −85 (O1) and −47 (O2) ppm. For CeO_2, the PBE result severely deviates from the reference line by −315 ppm, which can be significantly reduced to around only −5 ppm using the PBE+U with $U = 5$ eV. For readers' reference, a value of around 5 eV for the Hubbard U is commonly used in DFT+U electronic structure studies for rare-earth oxides [78–84]. We further investigate the reason for such dramatic changes on the PBE+U chemical shifts for these two materials. In Tables I and II, we tabulate the calculated shieldings decomposed into groups of isolated valence bands characterized by their atomic orbital signatures for La_2O_3 and CeO_2, respectively. Both tables indicate that the chemical shieldings, as well as the corresponding changes upon the Hubbard corrections, are dominated by the O-2p bands. More insightful information can be obtained by comparing the dominant component to their PBE/PBE+U density of states, as shown in Fig. 2. The figure tells us that the changes of the PBE+U chemical shifts originate from the coupling between O-2p and metallic 4f bands, due to the linear response. For La_2O_3, the La-5d bands are inert to the Hubbard term; however, a slightly downward shift can be found for Ce-5d bands which might result in noticeable contributions to the change of chemical shift through O-2p and Ce-5d couplings. Nevertheless, the large separations in energy between O-2p and Ce-5d bands has reduced the strength of the linear response coupling. This is verified by applying Hubbard U to Ce-5d orbitals instead and we found that, with $U = 5$ eV, it only results in 30 ppm changes in the chemical shift, about one-tenth of Ce-4f orbitals.

Finally, we would like to address the values of Hubbard U adopted in the selected materials. In the present study, unless otherwise mentioned above, the values of Hubbard U we adopted in our calculations can be found in literature [48,78–85], including calculated or empirical values. A particular case is the U value of La-4f, where we have used a

TABLE I. Calculated PBE/PBE+U ^{17}O chemical shielding (in ppm) for La_2O_3. Contributions are decomposed into groups of isolated bands indicated by their atomic characters. Values in the parentheses are the changes relative to the PBE result.

	La_2O_3 (O1)		La_2O_3 (O2)	
Bands	PBE	PBE+U	PBE	PBE+U
O-1s (core)	271.08	271.08	271.08	271.08
La-5s	−0.83	−0.81 (0.02)	−0.78	−0.77 (0.01)
O-2s	−5.88	−5.29 (0.59)	−5.07	−4.43 (0.64)
La-5p	20.01	17.46 (−2.55)	48.67	44.96 (−3.71)
O-2p	−646.73	−580.47 (66.26)	−760.82	−705.08 (55.74)
All	−362.35	−298.03 (64.32)	−446.92	−394.24 (52.68)

TABLE II. Calculated PBE/PBE+U ^{17}O chemical shielding (in ppm) for CeO_2. Contributions are decomposed into groups of isolated bands indicated by their atomic characters. Values in the parentheses are the changes relative to the PBE result.

	CeO_2	
Bands	PBE	PBE+U
O-1s (core)	271.08	271.08
Ce-5s	−1.10	−1.08 (0.02)
O-2s/Ce-5p	22.86	18.07 (−4.79)
O-2p	−1310.90	−997.62 (313.28)
All	−1018.06	−709.55 (308.51)

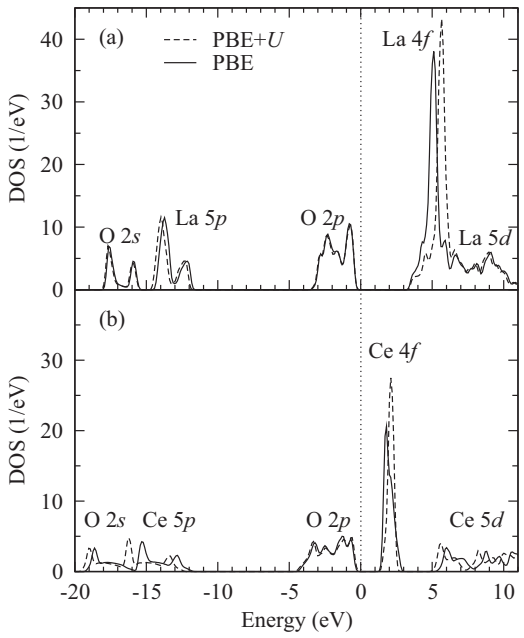

FIG. 2. Comparison of PBE and PBE+U total density of states for (a) La_2O_3 and (b) CeO_2. The major atomic characteristics are indicated near the spikes.

value of 2 eV fitting better to the regression lines. A value of 5 eV suggested by Ref. [78] will overshoot the corrections for the chemical shift in La_2O_3. In addition, we also found that, for each material, the changes of the chemical shifts due to the Hubbard term are incrementally correlated to the amount of the U values.

IV. CONCLUSIONS

In conclusion, we have adapted the DFT+U method into the GIPAW NMR chemical shift calculation. In order to incorporate the nonlocal Hubbard correction potential into the GIPAW Hamiltonian, the Hubbard potential has to comply with the GIPAW transformation. Before transforming the Hubbard potential, an extra phase is explicitly appended to the projector basis of the Hubbard potential which ensures the translational symmetry under an external uniform magnetic field. The induced current formulations for the chemical shift calculation have to be adjusted according to the DFT+U GIPAW Hamiltonian. Both the plane wave norm-conserving and ultrasoft versions of the DFT+U NMR calculation have been implemented. Since the Hubbard correction potential is nonlocal and orbital dependent, the derivations could provide some insights for further development of the GIPAW NMR method (e.g., with orbital dependent or nonlocal potentials).

The implementation has been applied to the ^{17}O chemical shift calculation for a selection of technically interesting materials, including transition-metal oxides and rare-earth oxides. For most of the studied oxides, the electronic structures are inappropriately determined by the LDA/PBE due to the presence of $3d$ or $4f$ localized electrons. A comparison of the calculated ^{17}O chemical shifts for these materials between the PBE and PBE+U is presented and discussed. For La_2O_3 and CeO_2, with physically reasonable U values, the implemented PBE+U approach is able to obtain more appropriate chemical shifts than the PBE approach, while for ZnO and TiO_2 polymorphs, the PBE chemical shift is sufficiently accurate. However, neither the PBE nor the PBE+U is able to provide a good description for Ti_2O_3. The present study also suggests that the GIPAW NMR chemical shift calculation provides an additional degree of freedom for validating the problematic exchange-correlation potentials used in DFT calculations.

ACKNOWLEDGMENTS

This work was supported by the Collaborative Computational Project for NMR Crystallography funded by the EPSRC (UK) Grants No. EP/J010510/1 and No. EP/M022501/1. The computation is provided by the high performance computing and modelling facility at Material Modelling Laboratory, Department of Materials, University of Oxford. B.-C. S. also acknowledges Prof. C. J. Pickard for discussions during the code development.

APPENDIX A: GIPAW METHOD AND THE HUBBARD POTENTIAL

In order to include the Hubbard correction potential in the GIPAW Hamiltonian, we need to ensure the translational invariance of Hubbard potential in the presence of a uniform magnetic field. In addition, the expression of the nonlocal Hubbard potential has to comply with the GIPAW transformation.

As an alternative view of understanding the additional phase in the GIPAW formulation, it is convenient to consider the translation of some atomic states. Without the presence of the magnetic field, the atomic states centering at position $\mathbf{R}_I$ are related to those at origin $\mathbf{R}_o$ by a translation operator so that we have

$$|\varphi_{\mathbf{R}_I,m}\rangle = e^{-i\mathbf{p}\cdot\mathbf{R}_I}|\varphi_{\mathbf{R}_o,m}\rangle. \tag{A1}$$

However, the expression of the translation operator is no longer accurate in the presence of an external uniform magnetic field. Instead, we can use the magnetic translation operator proposed by Brown [86] to obtain the correct expression. With the gauge origin at $\mathbf{R}_o$, the translation becomes

$$|\varphi_{\mathbf{R}_I,m}\rangle_{\mathbf{B}} = e^{-i(\mathbf{p}-\frac{1}{c}\mathbf{A}(\mathbf{r}))\cdot\mathbf{R}_I}|\varphi_{\mathbf{R}_o,m}\rangle = e^{\frac{i}{c}\mathbf{A}(\mathbf{r})\cdot\mathbf{R}_I}|\varphi_{\mathbf{R}_I,m}\rangle, \tag{A2}$$

where the subscript $\mathbf{B}$ indicates the presence of the magnetic field. It should be noticed that we have noted $|\varphi_{\mathbf{R}_o,m}\rangle_{\mathbf{B}} = |\varphi_{\mathbf{R}_o,m}\rangle$ at the gauge origin, and the translation generator is different from the familiar kinematic momentum $[\mathbf{p} + \frac{1}{c}\mathbf{A}(\mathbf{r})]$. Equation (A2) shows that the magnetic atomic states are related to their nonmagnetic ones with a position and vector potential dependent phase under a chosen gauge. Hence, consistent with the symmetric gauge used in previous GIPAW NMR articles where $\mathbf{A}(\mathbf{r}) = 1/2(\mathbf{B}\times\mathbf{r})$, the Hubbard potential in the presence of the magnetic field is written as

$$V_{\mathrm{HUB},\mathbf{B}} = \sum_I e^{\frac{i}{2c}\mathbf{r}\cdot\mathbf{R_I}\times\mathbf{B}} V^I_{\mathrm{HUB}} e^{\frac{-i}{2c}\mathbf{r}\cdot\mathbf{R_I}\times\mathbf{B}}. \tag{A3}$$

Applying the GIPAWtransformation to obtain the pseudoversion Hubbard potential, we can derive the GIPAW Hubbard potential as follows:

$$\begin{aligned}
\bar{V}_{\mathrm{HUB}} &= \mathcal{T}^{\mathrm{GIPAW}^\dagger} V_{\mathrm{HUB},\mathbf{B}} \mathcal{T}^{\mathrm{GIPAW}} \\
&= \mathcal{T}^{\mathrm{GIPAW}^\dagger}\mathcal{T}^{\mathrm{GIPAW}} \sum_{I\sigma mm'} e^{\frac{i}{2c}\mathbf{r}\cdot\mathbf{R_I}\times\mathbf{B}} U^{I,\sigma}_{m,m'} \\
&\quad \times |\tilde{\varphi}_{\mathbf{R}_I,m}\rangle\langle\tilde{\varphi}_{\mathbf{R}_I,m'}| e^{\frac{-i}{2c}\mathbf{r}\cdot\mathbf{R_I}\times\mathbf{B}} \mathcal{T}^{\mathrm{GIPAW}^\dagger}\mathcal{T}^{\mathrm{GIPAW}} \\
&= \sum_{I\sigma mm'} e^{\frac{i}{2c}\mathbf{r}\cdot\mathbf{R_I}\times\mathbf{B}} \left(U^{I,\sigma}_{m,m'} S^{(0)}|\tilde{\varphi}_{\mathbf{R}_I,m}\rangle\langle\tilde{\varphi}_{\mathbf{R}_I,m'}|S^{(0)}\right) \\
&\quad \times e^{\frac{-i}{2c}\mathbf{r}\cdot\mathbf{R_I}\times\mathbf{B}} \\
&\approx \tilde{V}_{\mathrm{HUB}} + \frac{1}{2c}\sum_I \mathbf{R}_I \times \frac{1}{i}\left[\mathbf{r}, \tilde{V}^I_{\mathrm{HUB}}\right]\cdot\mathbf{B},
\end{aligned} \tag{A4}$$

where the gauge phases between operators can be canceled out and $S_0 = (\mathcal{T}^{\mathrm{PAW}})^\dagger\mathcal{T}^{\mathrm{PAW}}$ is the overlap operator. The second and third GIPAW operators in the second equality of Eq. (A4) are responsible for transforming the pseudoatomic basis into the corresponding all-electron orbital basis of the Hubbard potential. In the last line, the exponential operators are expanded and approximated up to the first order of the magnetic field.

APPENDIX B: NUMERICAL VALIDATION

The commute of the position operator and the Hubbard potential (for short, the Hubbard commutator), $[\mathbf{r}, \tilde{V}^I_{\mathrm{HUB}}]/i$, appearing both in the velocity operator and the first-order perturbed Hamiltonian, is the major modification required for

TABLE III. Band gradients (in eV Å) calculated at $\mathbf{k} = (0.48,0.23,0.38)$ using numerical derivative ($\Delta\epsilon_n/\Delta k$) and velocity operator ($\hat{v}_{\mathrm{DFT}}$ and $\hat{v}_{\mathrm{DFT}+U}$) for *zb*-ZnO with PBE+U. The absolute calculated values are shown for the numerical derivative approach and only the relative and percentage (in the parentheses) errors are shown for the velocity operator approaches. Values calculated with velocity operator $\hat{v}_{DFT}$ exclude the contribution from the Hubbard commutator term.

Method	Band	NCPP			USPP		
		$\hat{x}$	$\hat{y}$	$\hat{z}$	$\hat{x}$	$\hat{y}$	$\hat{z}$
$\Delta\epsilon_n/\Delta k$	1	0.3491	0.0755	−0.0135	0.3777	0.0835	−0.0120
	2	−0.1135	0.2826	−0.1691	−0.1506	0.4132	−0.1196
	3	0.4362	−0.2511	0.2546	0.4872	−0.3036	0.2581
	4	0.4267	0.5702	−0.0930	0.5487	0.6218	−0.0890
	5	0.2981	−0.2296	0.3752	0.3236	−0.2251	0.3907
	6	1.0204	0.9129	0.1170	0.9979	0.8949	0.1065
	7	−1.1630	−2.0859	−2.2374	−1.3426	−2.2404	−2.3345
	8	−2.2029	−1.3656	1.8543	−2.2910	−1.4156	1.9278
	9	−2.3795	0.6793	0.0730	−2.4755	0.7058	0.0595
$\hat{v}_{\mathrm{DFT}}$	1	0.0885 (25.34)	0.0654 (87.19)	0.0253 (−187.10)	0.0768 (20.34)	0.0614 (73.55)	0.0247 (−197.23)
	2	0.0957 (−84.25)	−0.0928 (−32.84)	0.0335 (−19.78)	0.1139 (−75.64)	−0.1027 (−24.82)	0.0115 (−9.60)
	3	−0.0815 (−18.68)	0.0624 (−24.84)	−0.0535 (−21.01)	−0.0676 (−13.89)	0.0647 (−21.30)	−0.0442 (−17.13)
	4	−0.0451 (−10.58)	−0.0878 (−15.37)	0.0266 (−28.58)	−0.0407 (−7.42)	−0.0722 (−11.60)	0.0217 (−24.36)
	5	−0.0725 (−24.31)	0.0956 (−41.62)	−0.1024 (−27.30)	−0.0607 (−18.74)	0.0821 (−36.46)	−0.0828 (−21.19)
	6	−0.1609 (−15.76)	−0.1825 (−19.99)	0.0119 (10.15)	−0.1203 (−12.05)	−0.1398 (−15.62)	0.0178 (16.69)
	7	0.0274 (−2.35)	0.1212 (−5.81)	0.0836 (−3.73)	0.0116 (−0.86)	0.0965 (−4.30)	0.0625 (−2.67)
	8	0.0776 (−3.52)	0.0233 (−1.70)	−0.0182 (−0.98)	0.0606 (−2.64)	0.0170 (−1.19)	−0.0071 (−0.36)
	9	0.0980 (−4.11)	0.0110 (1.61)	−0.0077 (−10.56)	0.0748 (−3.02)	0.0145 (2.04)	−0.0057 (−9.65)
$\hat{v}_{\mathrm{DFT}}+U$	1	−0.0002 (−0.06)	−0.0002 (−0.21)	−0.0002 (1.18)	−0.0041 (−1.08)	−0.0022 (−2.59)	−0.0012 (10.08)
	2	0.0000 (0.03)	0.0004 (0.14)	0.0005 (−0.27)	−0.0062 (4.11)	0.0065 (1.58)	−0.0011 (0.92)
	3	0.0004 (0.09)	−0.0001 (0.02)	−0.0001 (−0.02)	0.0047 (0.96)	−0.0054 (1.76)	0.0013 (0.50)
	4	−0.0002 (−0.03)	0.0002 (0.02)	0.0005 (−0.48)	0.0055 (1.00)	0.0019 (0.30)	−0.0036 (4.06)
	5	−0.0001 (−0.04)	0.0002 (−0.10)	0.0002 (0.04)	0.0034 (1.06)	−0.0018 (0.81)	0.0041 (1.04)
	6	−0.0001 (−0.01)	0.0005 (0.05)	0.0001 (0.10)	−0.0023 (−0.23)	0.0017 (0.19)	−0.0003 (−0.24)
	7	0.0000 (−0.00)	0.0000 (0.00)	0.0002 (−0.00)	0.0024 (−0.18)	0.0026 (−0.11)	0.0009 (−0.03)
	8	0.0001 (−0.00)	0.0001 (−0.00)	0.0000 (0.00)	0.0012 (−0.05)	0.0000 (0.00)	−0.0007 (−0.03)
	9	0.0002 (−0.00)	−0.0001 (−0.01)	0.0002 (0.20)	0.0013 (−0.05)	0.0002 (0.03)	−0.0003 (−0.57)

the DFT+U induced current calculation. We have carefully examined the numerical accuracy for our DFT+U NMR chemical shift calculation by verifying the DFT+U band gradient and the numerical consistency among three chemical shift formulations as presented below.

1. Velocity operator

The augmented velocity operator, or equivalently the derivative of the Hamiltonian with respect to crystal momentum **k**, introduced in Sec. II C is one of the important operators in evaluating induced currents. The operator is also closely related to the calculation of the absorption spectrum in the electric dipole approximation. In the DFT+U version, extra contribution from the the Hubbard commutator has to be accounted for. In practical implementation, the expectation value is evaluated by using a modulation approach [60], which overcomes the ill-defined position operator in a periodic system. For the purpose of verifying the accuracy of the chemical shift calculation, we can examine the calculated band gradient.

Table III shows the calculated band gradients for the nine highest valence bands at $\mathbf{k} = (0.48,0.23,0.38)$ for zinc-blende phase ZnO (*zb*-ZnO). A nonspecial **k** point is chosen to avoid band crossings and $U = 7$ eV for the PBE+U. The band gradients are calculated by three approaches. First, the numerical approach calculates the band gradient directly by the change of the band energy with respect to a small shift in the **k** point, i.e., $\Delta\epsilon_n/\Delta k$. Second, the band gradients are calculated using the velocity operator without the Hubbard commutator, $\hat{v}_{\mathrm{DFT}}$. And third, the calculation is carried out using the velocity operator in the DFT+U formulation, $\hat{v}_{\mathrm{DFT}+U}$. The results evaluated from the latter two approaches are compared with the first one whose values are supposed to be exact. In summary, the velocity operator results are most accurate, with the error less than 0.1%, in the case of the DFT+U velocity operator approach with norm-conserving pseudopotentials. A slight increase of error (up to a few percent) can be found when using the ultrasoft pseudopotentials. The source of errors has been identified originating from the deviations of the direct product of the PAW projector functions (in the overlap matrix) and the atomic orbital functions (in the Hubbard potential) in which both functions have been conveniently interpolated in the reciprocal space. In the next subsection, we further verified that the error in the ultrasoft pseudopotential plays only insignificant variations in the chemical shift results. Nevertheless, the error can increase substantially to several tens of percent if the contributions from the Hubbard commutator is ignored, as shown in the $\hat{v}_{\mathrm{DFT}}$ section in Table III.

TABLE IV. PBE and PBE+U chemical shieldings for nuclei in TiO_2 and $TiCl_4$ molecules. For comparison, results are calculated with norm-conserving and ultrasoft pseudopotentials using various induced current formulations.

System	Site	Approach	PBE		PBE+U	
			NCPP	USPP	NCPP	USPP
TiO_2		Crystal	−383.48	−379.00	−338.28	−329.13
	^{47}Ti	Molecular	−383.67	−379.38	−338.46	−329.62
		Sum rule	−383.66	−379.46	−338.45	−329.64
		Crystal	−843.49	−838.86	−753.66	−750.49
	^{17}O	Molecular	−843.81	−839.12	−753.96	−750.71
		Sum rule	−843.72	−838.80	−753.87	−750.39
$TiCl_4$		Crystal	−971.57	−930.20	−973.78	−936.64
	^{47}Ti	Molecular	−971.60	−930.85	−973.84	−937.33
		Sum rule	−971.60	−930.94	−973.84	−937.41
		Crystal	−958.46	−988.17	−905.44	−936.27
	^{35}Cl	Molecular	−958.87	−988.53	−905.89	−936.57
		Sum rule	−958.87	−988.53	−905.89	−936.57

2. Molecular and crystal approaches

In the GIPAW NMR chemical shift calculation, the response currents are formulated into three approaches: molecular, molecular with sum rule, and crystal approaches [7,28]. Calculations for periodic systems are restricted to the crystal approach; however, molecular calculations can be simulated with crystal approach using the supercell technique. For both molecular approaches, the position operator in the induced current calculation has been replaced by a sawtooth function antisymmetrically at the geometric center of a molecule. A generalized f-sum rule [7,28] has been utilized to convert the molecular approach into the molecular sum rule approach. During the conversion, a commutator term in both bare and paramagnetic correction currents has been converted into the velocity operator. We use this property to justify the negligence band-gradient error in the ultrasoft potential case for chemical shift calculations. While in the crystal approach, which is extended from the molecular sum rule formulation, auxiliary functions have been devised to replace the ill-defined position operator. Detailed derivations can be found in the original GIPAW papers [7,28].

For completeness, the DFT+U induced current has been adapted in the aforementioned three approaches. We have verified the implementation by examining the consistency of chemical shieldings among three approaches. The calculations are performed on the TiO_2 and $TiCl_4$ molecules using PBE/PBE+U ($U = 3$ eV) and geometrically optimized in a large cubic cell (volume = 1000 Å^3). The calculated isotropic chemical shieldings, σ_{iso}, for all types of nuclei are tabulated in Table IV. It shows that the calculated chemical shieldings are consistent among the three approaches, with the errors within 1 ppm either using the DFT or DFT+U. The consistency has verified the gauge invariant criterion for the formulations. In addition, the extreme agreements between the molecular and the molecular sum-rule approaches suggest the negligible error arising from the Hubbard commutator evaluated with the ultrasoft pseudopotentials.

[1] Z. Gan, P. Gor'kov, T. A. Cross, A. Samoson, and D. Massiot, J. Am. Chem. Soc. **124**, 5634 (2002).
[2] S. E. Ashbrook, Phys. Chem. Chem. Phys. **11**, 6892 (2009).
[3] A. Lesage, Phys. Chem. Chem. Phys. **11**, 6876 (2009).
[4] J. Hanna and M. Smith, Solid State Nucl. Magn. Reson. **38**, 1 (2010).
[5] C. Bonhomme, C. Gervais, F. Babonneau, C. Coelho, F. Pourpoint, T. Azaïs, S. E. Ashbrook, J. M. Griffin, J. R. Yates, F. Mauri *et al.*, Chem. Rev. **112**, 5733 (2012).
[6] S. E. Ashbrook and S. Sneddon, J. Am. Chem. Soc. **136**, 15440 (2014).
[7] C. J. Pickard and F. Mauri, Phys. Rev. B **63**, 245101 (2001).
[8] P. Hohenberg and W. Kohn, Phys. Rev. **136**, B864 (1964).
[9] W. Kohn and L. J. Sham, Phys. Rev. **140**, A1133 (1965).
[10] T. Charpentier, Solid State Nucl. Magn. Reson. **40**, 1 (2011).
[11] S. J. Clark, M. D. Segall, C. J. Pickard, P. J. Hasnip, M. I. J. Probert, K. Refson, and M. C. Payne, Z. Kristallogr.–Cryst. Mater. **220**, 567 (2005).
[12] http://www.nersc.gov/users/software/applications/materials science/paratec/.
[13] P. Blaha, K. Schwarz, P. Sorantin, and S. Trickey, Comput. Phys. Commun. **59**, 399 (1990).
[14] P. Blaha, K. Schwarz, G. K. H. Madsen, D. Kvasnicka, and J. Luitz, *An Augmented Plane Wave Plus Local Orbital Program for Calculating Crystal Properties* (Vienna University of Technology, Vienna, 2001).
[15] P. Giannozzi, S. Baroni, N. Bonini, M. Calandra, R. Car, C. Cavazzoni, D. Ceresoli, G. L. Chiarotti, M. Cococcioni, I. Dabo *et al.*, J. Phys.: Condens. Matter **21**, 395502 (2009).
[16] G. Kresse and J. Furthmüller, Phys. Rev. B **54**, 11169 (1996).
[17] D. Skachkov, M. Krykunov, E. Kadantsev, and T. Ziegler, J. Chem. Theory Comput. **6**, 1650 (2010).
[18] D. Skachkov, M. Krykunov, and T. Ziegler, Can. J. Chem. **89**, 1150 (2011).
[19] R. Laskowski and P. Blaha, Phys. Rev. B **85**, 245117 (2012).
[20] D. Sebastiani and M. Parrinello, J. Phys. Chem. A **105**, 1951 (2001).
[21] T. Thonhauser, D. Ceresoli, A. A. Mostofi, N. Marzari, R. Resta, and D. Vanderbilt, J. Chem. Phys. **131**, 101101 (2009).
[22] C. G. Van de Walle and P. E. Blöchl, Phys. Rev. B **47**, 4244 (1993).
[23] C. J. Pickard and F. Mauri, Phys. Rev. Lett. **88**, 086403 (2002).
[24] H. M. Petrilli, P. E. Blöchl, P. Blaha, and K. Schwarz, Phys. Rev. B **57**, 14690 (1998).
[25] M. Profeta, F. Mauri, and C. J. Pickard, J. Am. Chem. Soc. **125**, 541 (2002).
[26] S. A. Joyce, J. R. Yates, C. J. Pickard, and F. Mauri, J. Chem. Phys. **127**, 204107 (2007).
[27] T. F. G. Green and J. R. Yates, J. Chem. Phys. **140**, 234106 (2014).
[28] J. R. Yates, C. J. Pickard, and F. Mauri, Phys. Rev. B **76**, 024401 (2007).

[29] J. P. Perdew and Y. Wang, Phys. Rev. B **33**, 8800 (1986).
[30] L. J. Sham and M. Schlüter, Phys. Rev. Lett. **51**, 1888 (1983).
[31] J. P. Perdew and M. Levy, Phys. Rev. Lett. **51**, 1884 (1983).
[32] J. P. Perdew and A. Zunger, Phys. Rev. B **23**, 5048 (1981).
[33] R. Laskowski, P. Blaha, and F. Tran, Phys. Rev. B **87**, 195130 (2013).
[34] V. I. Anisimov, J. Zaanen, and O. K. Andersen, Phys. Rev. B **44**, 943 (1991).
[35] V. I. Anisimov, I. V. Solovyev, M. A. Korotin, M. T. Czyzyk, and G. A. Sawatzky, Phys. Rev. B **48**, 16929 (1993).
[36] O. Gunnarsson, O. K. Andersen, O. Jepsen, and J. Zaanen, Phys. Rev. B **39**, 1708 (1989).
[37] V. I. Anisimov and O. Gunnarsson, Phys. Rev. B **43**, 7570 (1991).
[38] W. E. Pickett, S. C. Erwin, and E. C. Ethridge, Phys. Rev. B **58**, 1201 (1998).
[39] N. J. Mosey, P. Liao, and E. A. Carter, J. Chem. Phys. **129**, 014103 (2008).
[40] F. Aryasetiawan, M. Imada, A. Georges, G. Kotliar, S. Biermann, and A. I. Lichtenstein, Phys. Rev. B **70**, 195104 (2004).
[41] F. Aryasetiawan, K. Karlsson, O. Jepsen, and U. Schönberger, Phys. Rev. B **74**, 125106 (2006).
[42] I. V. Solovyev and M. Imada, Phys. Rev. B **71**, 045103 (2005).
[43] T. Miyake and F. Aryasetiawan, Phys. Rev. B **77**, 085122 (2008).
[44] T. Miyake, F. Aryasetiawan, and M. Imada, Phys. Rev. B **80**, 155134 (2009).
[45] K. Karlsson, F. Aryasetiawan, and O. Jepsen, Phys. Rev. B **81**, 245113 (2010).
[46] E. Şaşıoğlu, C. Friedrich, and S. Blügel, Phys. Rev. B **81**, 054434 (2010).
[47] E. Şaşıoğlu, C. Friedrich, and S. Blügel, Phys. Rev. B **83**, 121101 (2011).
[48] B.-C. Shih, Y. Zhang, W. Zhang, and P. Zhang, Phys. Rev. B **85**, 045132 (2012).
[49] Y. Nomura, M. Kaltak, K. Nakamura, C. Taranto, S. Sakai, A. Toschi, R. Arita, K. Held, G. Kresse, and M. Imada, Phys. Rev. B **86**, 085117 (2012).
[50] M. Cococcioni and S. de Gironcoli, Phys. Rev. B **71**, 035105 (2005).
[51] S. Baroni, S. de Gironcoli, A. Dal Corso, and P. Giannozzi, Rev. Mod. Phys. **73**, 515 (2001).
[52] P. E. Blöchl, Phys. Rev. B **50**, 17953 (1994).
[53] R. Ditchfield, J. Chem. Phys. **56**, 5688 (1972).
[54] A. I. Liechtenstein, V. I. Anisimov, and J. Zaanen, Phys. Rev. B **52**, R5467(R) (1995).
[55] S. L. Dudarev, G. A. Botton, S. Y. Savrasov, C. J. Humphreys, and A. P. Sutton, Phys. Rev. B **57**, 1505 (1998).
[56] O. Bengone, M. Alouani, P. Blöchl, and J. Hugel, Phys. Rev. B **62**, 16392 (2000).
[57] B. Amadon, F. Jollet, and M. Torrent, Phys. Rev. B **77**, 155104 (2008).
[58] G. Trimarchi and N. Binggeli, Phys. Rev. B **71**, 035101 (2005).
[59] M. T. Czyzyk and G. A. Sawatzky, Phys. Rev. B **49**, 14211 (1994).
[60] C. J. Pickard and M. C. Payne, Phys. Rev. B **62**, 4383 (2000).
[61] T. Gregor, F. Mauri, and R. Car, J. Chem. Phys. **111**, 1815 (1999).
[62] D. S. Middlemiss, F. Blanc, C. J. Pickard, and C. P. Grey, J. Magn. Reson. **204**, 1 (2010).
[63] J. P. Perdew, K. Burke, and M. Ernzerhof, Phys. Rev. Lett. **77**, 3865 (1996).
[64] M. Profeta, M. Benoit, F. Mauri, and C. J. Pickard, J. Am. Chem. Soc. **126**, 12628 (2004).
[65] T. Bastow and S. Stuart, Chem. Phys. **143**, 459 (1990).
[66] S. Yang, J. Shore, and E. Oldfield, J. Magn. Reson. (1969) **99**, 408 (1992).
[67] T. J. Bastow, A. F. Moodie, M. E. Smith, and H. J. Whitfield, J. Mater. Chem. **3**, 697 (1993).
[68] T. J. Bastow, G. Doran, and H. J. Whitfield, Chem. Mater. **12**, 436 (2000).
[69] H. J. Monkhorst and J. D. Pack, Phys. Rev. B **13**, 5188 (1976).
[70] S. Z. Karazhanov, P. Ravindran, A. Kjekshus, H. Fjellvåg, and B. G. Svensson, Phys. Rev. B **75**, 155104 (2007).
[71] R. Laskowski and P. Blaha, J. Phys. Chem. C **119**, 731 (2015).
[72] S. H. Shin, G. V. Chandrashekhar, R. E. Loehman, and J. M. Honig, Phys. Rev. B **8**, 1364 (1973).
[73] K. E. Smith and V. E. Henrich, Phys. Rev. B **38**, 5965 (1988).
[74] L. F. Mattheiss, J. Phys.: Condens. Matter **8**, 5987 (1996).
[75] A. I. Poteryaev, A. I. Lichtenstein, and G. Kotliar, Phys. Rev. Lett. **93**, 086401 (2004).
[76] V. Eyert, U. Schwingenschlögl, and U. Eckern, Europhys. Lett. **70**, 782 (2005).
[77] Y. Guo, S. J. Clark, and J. Robertson, J. Phys.: Condens. Matter **24**, 325504 (2012).
[78] S. Fabris, S. de Gironcoli, S. Baroni, G. Vicario, and G. Balducci, Phys. Rev. B **71**, 041102 (2005).
[79] N. Singh, S. M. Saini, T. Nautiyal, and S. Auluck, J. Appl. Phys. **100**, 083525 (2006).
[80] C. Loschen, J. Carrasco, K. M. Neyman, and F. Illas, Phys. Rev. B **75**, 035115 (2007).
[81] D. A. Andersson, S. I. Simak, B. Johansson, I. A. Abrikosov, and N. V. Skorodumova, Phys. Rev. B **75**, 035109 (2007).
[82] J. L. F. Da Silva, Phys. Rev. B **76**, 193108 (2007).
[83] H. Jiang, R. I. Gomez-Abal, P. Rinke, and M. Scheffler, Phys. Rev. Lett. **102**, 126403 (2009).
[84] J. Kullgren, C. W. M. Castleton, C. Müller, D. M. Ramo, and K. Hermansson, J. Chem. Phys. **132**, 054110 (2010).
[85] M. E. Arroyo-de Dompablo, A. Morales-García, and M. Taravillo, J. Chem. Phys. **135**, 054503 (2011).
[86] E. Brown, Phys. Rev. **133**, A1038 (1964).